Original Research Article

Virtual Screening of FDA Approved Drugs Library to Identify a Potential Inhibitor Against NS2B-NS3 Protease of Yellow Fever Virus.

Abstract:

Yellow fever is a neglected hemorrhagic disease with a high case fatality rate ranging between 25% and 50% for the hospitalized patients. Yellow fever disease is caused by a zoonotic pathogen known as yellow fever virus. This RNA virus is usually transmitted by mosquitos and it is considered endemic in the tropical regions of South America and Africa. Although an effective vaccine is available for yellow fever virus, no antiviral drug is yet licensed against the disease. Thus, yellow fever virus is still representing a re-emerging threat among unvaccinated individuals in endemic regions. The NS2B-NS3 protease seems to play an important role in yellow fever virus replication cycle. As such, the NS2B-NS3 protease may represent a potential target for structure-based drug design and discovery. In this direction, computational approaches like virtual screening can be utilized to hasten the design of novel antivirals and/ or repurposing an already FDA approved drugs. In this in silico study, an FDA approved drugs library was screened against NS2B-NS3 protease crystal of yellow fever virus. Then the best hits with least energy of binding and ability of hydrogen bonding with key residues of protease active site were then selected and submitted to molecular dynamics simulation. And throughout simulation interval, only Olsalazine was able to stay in close proximity to the active site of protease crystal with least average MM-PBSA binding energy as compared to Dantrolene, Belinostat and Linezolid. This indicates that Olsalazine may have the best capacity to bind to NS2B-NS3 protease and interfere with its activity.

Keywords: yellow fever virus, NS2B-NS3 protease, FDA approved drugs, repurposing, virtual screening.

Introduction:

Yellow fever (YF) is a viral hemorrhagic disease caused by a zoonotic pathogen known as yellow fever virus (YFV) [1]. Yellow fever is considered a mosquito-borne disease that is mostly common in the tropical zones of South America and Africa [2]. The causative pathogen, yellow fever virus, has a positive-sense and single-stranded RNA genome. Yellow fever virus belongs to the family *Flaviviridae* and it is a prototypical member of the *Flavivirus* genus. In addition to YFV, The *Flavivirus* genus does include other important pathogenic viruses like Zika virus and dengue virus [3]. YFV infection can produce a wide spectrum of manifestations that can range from completely asymptomatic to severe hemorrhagic fever. For hospitalized patients with severe yellow fever disease, the case fatality rate is high and ranging between 25% and 50% [4,5]. Infection with YFV can be diagnosed through viral culture, RNA detection and detection of YFV-antibodies by serological tests [6]. Currently, no antiviral therapy is available against YFV and prevention approaches are mainly dependent on the use of 17D live attenuated vaccine as a single dose [1,7]. Although YFV-17D vaccine is highly effective, both limited vaccine production capacity and low number of vaccinated people make YFV a real challenge for public health in endemic regions. The possibility of this public health threat was recently confirmed during Angola and Brazil outbreaks of YFV [1,8,9]. YF is considered a neglected tropical disease as it attracts a relatively limited research interest. As a result, many facets of YFV biology are not fully understood like host range and interactions between host and virus [1,10]. Therefore, it is of interest to design antiviral tools capable of curbing any resurgence of YFV in endemic regions. In this direction, attempts to repurpose Ribavirin and Sofosbuvir against YFV were promising during in vitro studies and mouse models evaluation. However, these encouraging findings for Ribavirin couldn't be replicated in non-human primates [11,12]. The genome of YFV encodes a single polyprotein that is cleaved later by cellular and viral proteases into three structural proteins and seven nonstructural (NS) proteins. The structural proteins include capsid (C), envelope (E) and membrane (M) proteins and they are important for viral particles formation. While nonstructural proteins (NS) are essential for virus replication machinery, and these proteins namely are NS1, NS2A, NS2B, NS3, NS4A, NS4B, NS5 [13]. The amino terminus of NS3 is considered a typical serine protease and it needs NS2B as a cofactor. The NS2B-NS3 protease is considered essential for YFV replicative machinery and represents a potential target for the development of antiviral candidates [14,15]. A three-dimensional representation for NS2B-NS3 protease of YFV can be seen in Figure 1.

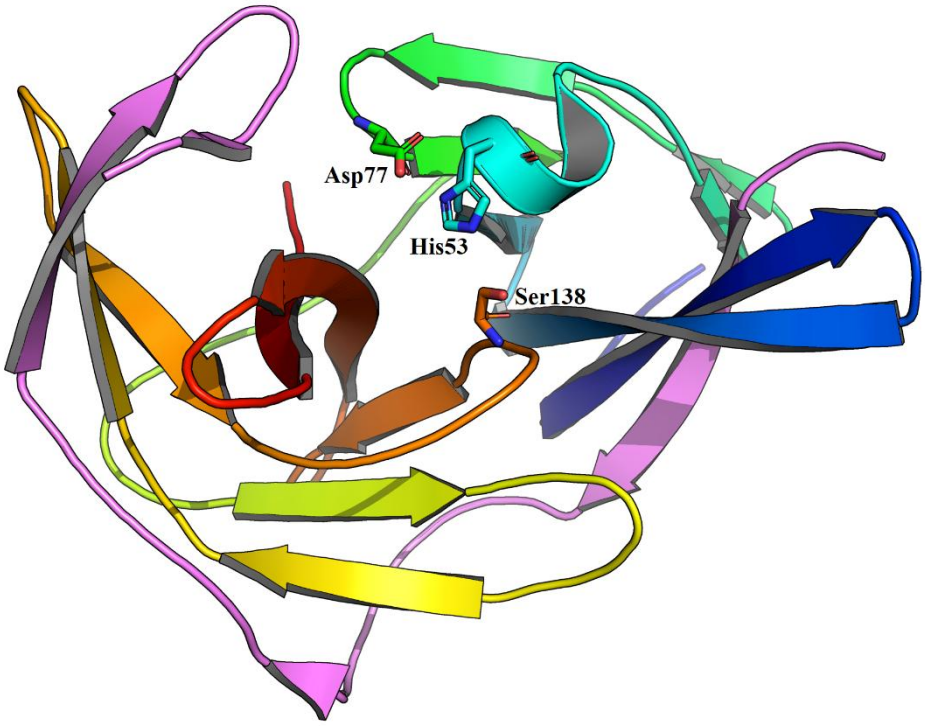

Figure 1: A three-dimensional illustration of YFV NS2B-NS3 protease (PDB: 6URV). NS3 chain is colored with rainbow gradient where the C-terminus is shown in red and N-terminus is displayed in blue. While NS2B chain is colored with violet. Key residues of protease active site in NS3 chain are shown as labelled sticks.

Virtual screening (VS) approach is widely employed nowadays to save both time and cost of drug development projects. In virtual screening, both structural and physico-chemical properties of ligands and/ or target proteins are utilized to generate a predictive model. The generated model can be then used to identify novel lead molecules and repurpose approved drugs [16]. In this study, we have virtually screened a library of 1615 FDA approved drugs from ZINC database against NS2B-NS3 protease crystal of YFV. The goal of this in silico study is to repurpose approved drugs as possible inhibitors of YFV NS2B-NS3 protease.

Methodology:

- Setting up a plan for virtual screening study:

An overview for this screening study is outlined in Figure 2. As seen in this figure, the main steps of this study are similar to what we had employed in our previous virtual screening studies [17,18]. In summary, a library of FDA approved drugs was screened against NS2B-

NS3 protease crystal of YFV by using docking program. According to docking results, the top ten hits with minimum energy of binding were selected for further evaluation. Then we have picked out, of these ten hits, only those drugs with ability to form a hydrogen bond with key residues of protease active site. Finally, only those hits with minimum docking energy of binding and capacity of hydrogen bonding were subjected to molecular dynamics (MD) study.

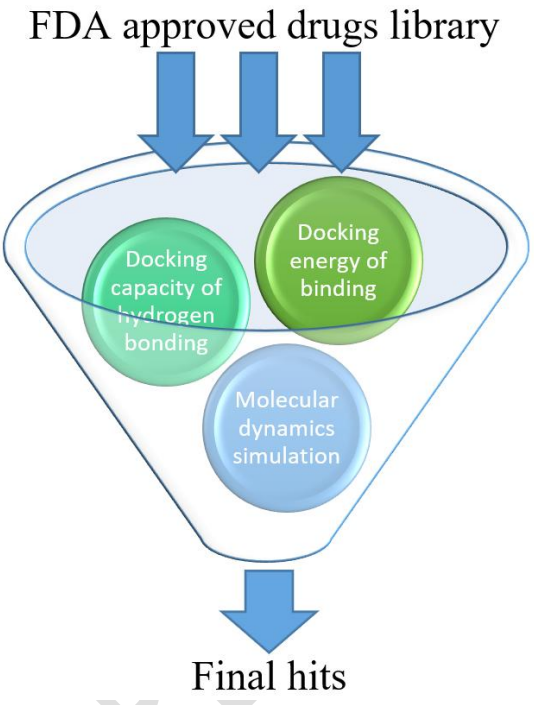

Figure 2: A concise illustration for virtual screening study plan.

- Structure-based virtual screening (SBVS):

A library of 1,615 FDA approved drugs was downloaded in SDF format from ZINC 15 database [19,20]. This library was then uploaded into an online drug discovery platform named Mcule.com [21]. After uploading FDA approved drugs library, these drugs were screened against NS2B-NS3 protease crystal of YFV. This protease crystal, with PDB code of 6URV, was obtained from Protein Data bank [22,23]. For simplicity of screening, only chains A and B of NS2B-NS3 protease crystal were used while other chains were deleted by using USCF chimera version 1.15 [24]. Upon uploading the protease crystal, Mcule.com automatically prepared the crystal for docking by using AutoDock tools [25]. The structure-based virtual screening (SBVS) in Mcule.com was carried out by using an embedded version of AutoDock Vina [26], default parameters were used for this virtual screening study. The docking coordinates were (X= -3.0, Y= 1.0, Z= 7.0) and the binding site area was (22*22*22)

Angstrom. After docking was finished, the hits were ranked based on their minimum energy of binding. Only the top ten hits with least energy of binding were then selected for further evaluation. First, we have explored the clinical indications and legal status of dispensing for these top hits by using Medscape.com online reference [27]. Then for each of these ten hits, the ligand-protease complex with least energy of binding pose was assessed for formation of hydrogen bonds between ligand and key residues of protease active site by using LigPlot^{+} v2.2.4 [28]. Finally, only those hits with minimum docking energy of binding and capacity of hydrogen bonding were then submitted to molecular dynamics (MD) simulation.

- Molecular dynamics (MD) simulation:

For the selected hits of virtual screening, MD study was carried out for 100 nanoseconds by using YASARA Dynamics v20.12.24 [29]. For each of these hits, the ligand-protease complex with minimum energy of binding pose was submitted as PDB format to MD simulation. In this MD study, the hydrogen bonds were optimized and the pKa value was predicted in order to fine-tune the amino acids protonation at pH = 7.4 [30]. Sodium chloride (NaCl) was used in this MD simulation with a concentration of 0.9%, an additional concentration of either sodium or chloride was used to neutralize the complex of ligand and protease. Also, minimizations of steepest descent and simulated annealing were employed to get rid of any probable clashes during simulation. For this simulation, the used force fields include AM1BCC and GAFF2 for the ligand, TIP3P for the water and AMBER14 for the solute [31–33]. For the AMBER force field, default parameters were employed, the cutoff limit for van der Waals (vdW) forces was 8 Angstrom [34]. On the other hand, no cutoff limit was used for electrostatic forces due to the implementation of Particle Mesh Ewald algorithm [35]. For bonded and non-bonded interactions, motions equations were used as multiple timesteps of 1.25 femtoseconds and 2.5 femtoseconds respectively at a pressure of 1 atm and temperature of 298K [36]. Then after assessment of Root Mean Square Deviation (RMSD) for the solute as a function of simulation duration, the first 100 nanoseconds duration was considered as the equilibrium time and precluded from additional analysis. Finally, GraphPad Prism v8.0.2 was used to plot and visualize movement RMSD and conformation RMSD of the ligand throughout simulation period.

By using AMBER14 force field, a built-in macro in YASARA Dynamics was used for the calculation of Molecular Mechanics Poisson-Boltzmann Surface Area (MM-PBSA) binding

energy [37]. The YASARA Dynamics can calculate MM-PBSA binding energy by using the following equation:

$$\text{Binding Energy} = \text{EpotRecept} + \text{EsolvRecept} + \text{EpotLigand} + \text{EsolvLigand} - \text{EpotComplex} - \text{EsolvComplex}$$

Results and discussion:

As mentioned before, we have selected the top ten hits for the virtual screening of FDA drugs library against NS2B-NS3 protease of YFV. These best ten hits can be seen in Table 1 where they were ordered according to their minimum energy of binding to protease active site. An overview for the chemical and clinical features of these top hits can be seen in Table 1. According to Medscape.com online reference, all these ten hits are considered prescription only medications [27]. As can be noticed in Table 1, the muscle relaxant drug (Dantrolene) has the least docking energy of binding to YFV protease. Dantrolene was suggested as a potential inhibitor of papain-like proteinase (PL^{pro}) for severe acute respiratory syndrome coronavirus 2 (SARS-CoV-2) according to a molecular docking study [38]. Another review study has proposed that the use of Dantrolene may minimize morbidity and mortality associated with coronavirus disease 2019 (COVID-19) through restoring calcium ions homeostasis. By lowering the release of Ca^{2+} from endoplasmic reticulum, Dantrolene may have the potential to reduce inflammation, oxidative stress and apoptosis usually associated with severe COVID-19 [39]. Then the third best hit in Table 1, Pomalidomide, is licensed by FDA for the management of multiple myeloma [27]. Pomalidomide is a pyridone-containing drug and it may have the ability to inhibit SARS-CoV-2 main protease (M^{pro}) according to a previous docking study [40]. The anti-inflammatory agent (Olsalazine) can be seen in Table 1 as the fifth best potential ligand to YFV protease crystal. Olsalazine may have a good binding capacity to SARS-CoV-2 M^{pro} based on a recent in silico screening study, however Olsalazine appears to lose contact with M^{pro} catalytic site in molecular dynamics simulation [41]. The seventh best hit in Table 1 is the antifungal agent (Naftifine), it is a naphthyl-based drug with known capacity to inhibit SARS-CoV PL^{pro} [42]. Finally, the eighth hit in Table 1 is the diuretic agent (Chlorothiazide) and it may have a good affinity against SARS-CoV-2 PL^{pro} according to an in silico study [43].

Table 1: Summary of chemical and clinical characteristics of the top ten hits that were virtually screened against NS2B-NS3 protease of yellow fever virus. These drugs were ranked based on their minimum energy of binding to the crystal of NS2B-NS3 protease.

No.	Generic name	Molecular formula	Energy of binding (Kcal/ mol)	Indications	Legal status
1	Dantrolene	$C_{14}H_{10}N_4O_5$	-5.9	Malignant hyperthermia, muscle spasticity	POM
2	Belinostat	$C_{15}H_{14}N_2O_4S$	-5.6	Peripheral T-cell lymphoma	POM
3	Pomalidomide	$C_{13}H_{11}N_3O_4$	-5.4	Multiple myeloma	POM
4	Anagrelide	$C_{10}H_7Cl_2N_3O$	-5.4	Thrombocythemia	POM
5	Olsalazine	$C_{14}H_{10}N_2O_6$	-5.2	Ulcerative colitis	POM
6	Rosiglitazone	$C_{18}H_{19}N_3O_3S$	-5.0	Type 2 diabetes mellitus	POM
7	Naftifine	$C_{21}H_{21}N$	-5.0	Dermatophytosis	POM
8	Chlorothiazide	$C_7H_6ClN_3O_4S_2$	-5.0	Hypertension, edema	POM
9	Linezolid	$C_{16}H_{20}FN_3O_4$	-5.0	Gram-positive bacterial infection	POM
10	Methoxsalen	$C_{12}H_8O_4$	-5.0	Vitiligo, psoriasis	POM

POM: Prescription only medication.

Next, the best ten hits of the virtual screening were assessed for their ability to interact with key residues of NS2B-NS3 protease active site for YFV. The amino terminus of NS3 protein is considered a serine protease, the key residues of the active site for this protease are histidine 53, asparagine 77 and serine 138. The NS3 protease activity requires NS2B protein as a cofactor subunit [13]. Thus, the ability of the virtual screening hits to form hydrogen bonds with key residues of NS2B-NS3 protease active site may reflect better capacity of these hits to interfere with protease activity. A summary of molecular docking study for the top ten hits against YFV protease crystal can be seen in Table 2. Again, in this table, these ten hits were ordered according to their minimum energy of binding to protease crystal. Table 2 shows the ability of each hit to form hydrogen bonds with the three key residues of protease active site. As seen in Table 2, only four drugs were able to form hydrogen bonds with key

residues of YFV protease active site and these drugs are Dantrolene, Belinostat, Olsalazine and Linezolid. These four drugs were able to form a hydrogen bond with serine 138 in NS3 chain of protease crystal as seen in Table 2 and Figure 3. In Figure 3, a two-dimensional illustration can be seen for the docking of these four drugs against NS2B-NS3 protease. Both Dantrolene and Linezolid were able to form a hydrogen bond with serine 138 residue and the length of this hydrogen bonds was less than 3.0 Angstrom, as can be seen in Figure 3. Then, for each of these four drugs, the ligand-protease complex with least energy of binding pose was submitted for MD simulation for 100 nanoseconds.

Table 2: Summary of docking study for the best ten hits against NS2B-NS3 protease of yellow fever virus.

No.	Drug name	Vina energy of binding (Kcal/ mol)	Capacity of hydrogen bonding with key residues of protease active site		
			His 53	Asp 77	Ser 138
1	Dantrolene	-5.9	No	No	Yes
2	Belinostat	-5.6	No	No	Yes
3	Pomalidomide	-5.4	No	No	No
4	Anagrelide	-5.4	No	No	No
5	Olsalazine	-5.2	No	No	Yes
6	Rosiglitazone	-5.0	No	No	No
7	Naftifine	-5.0	No	No	No
8	Chlorothiazide	-5.0	No	No	No
9	Linezolid	-5.0	No	No	Yes
10	Methoxsalen	-5.0	No	No	No

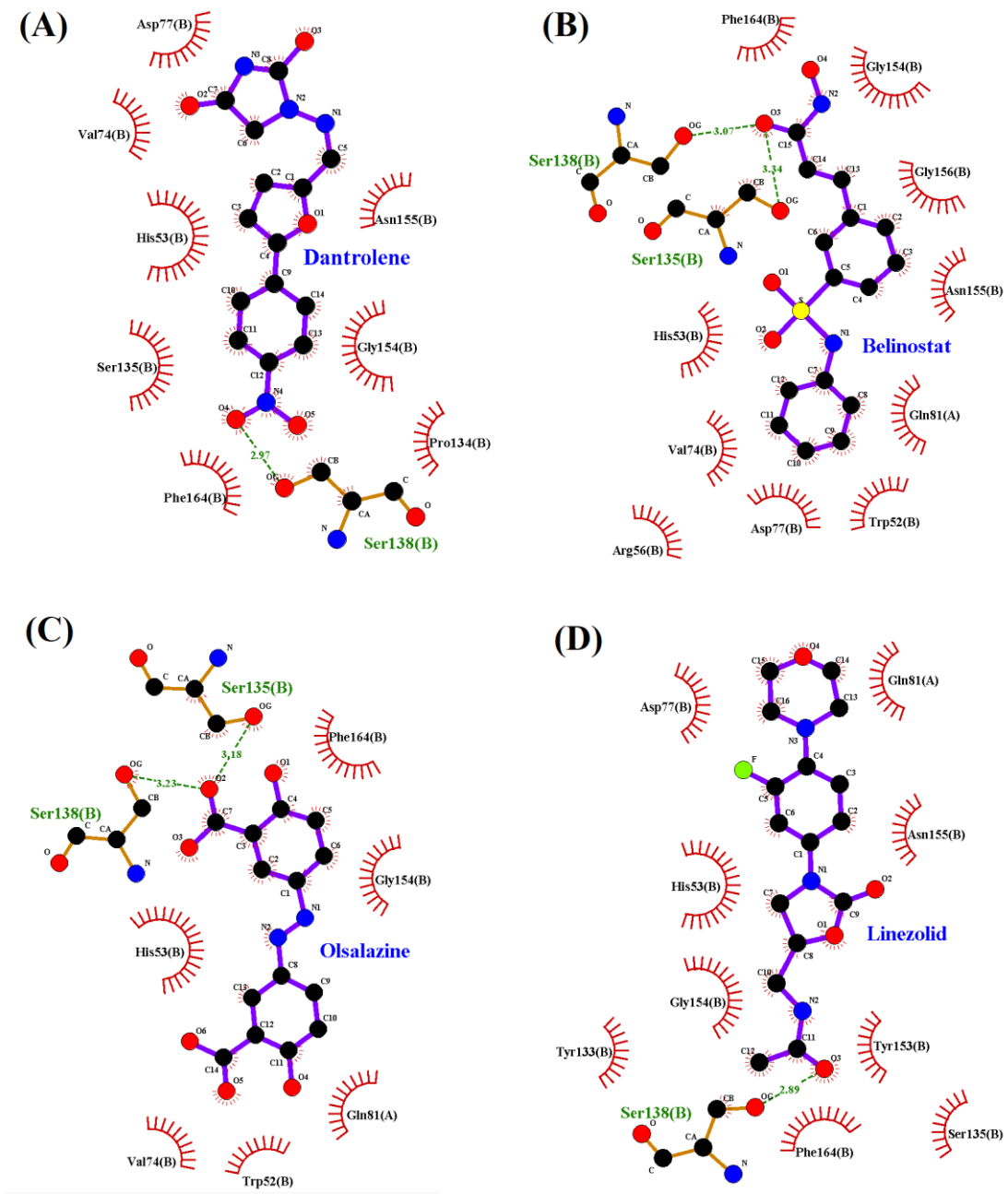

Figure 3: Two-dimensional illustrations for docking of (A) Dantrolene, (B) Belinostat, (C) Olsalazine and (D) Linezolid against NS2B-NS3 protease of YFV. The atoms of carbon, oxygen, nitrogen and sulfur are colored by black, red, blue and yellow respectively. Hydrophobic interactions are represented as small multiple red lines while hydrogen bonds are shown as green dashed line.

A summary for molecular dynamics (MD) simulation report can be seen in both Figure 4 and Table 3. By superposing the protease-ligand complex on its reference structure throughout

simulation period, the proximity of the ligand to protease active site can be estimated. As can be seen in Figure 4 and Table 3, both Belinostat and Linezolid failed to maintain close proximity to protease active site with mean ligand movement RMSD of 24.06 and 33.55 Angstrom respectively. A fluctuation in Dantrolene movement RMSD can be observed in Figure 4 in the beginning and the end of simulation with mean RMSD of 6.12 Angstrom as seen in Table 3. Finally, Olsalazine showed the closest and the most constant proximity to protease active site with a mean ligand movement RMSD of 4.59 Angstrom.

The estimation of average MM-PBSA binding energy, as reported in Table 3, seems to be in full agreement with mean ligand movement RMSD for each of the four selected hits. Again, the least average MM-PBSA binding energy was reported for Olsalazine followed by Dantrolene, Belinostat and finally Linezolid. These simulation results indicate that Olsalazine may have the best binding capacity to YFV protease active site as compared to the other three drugs.

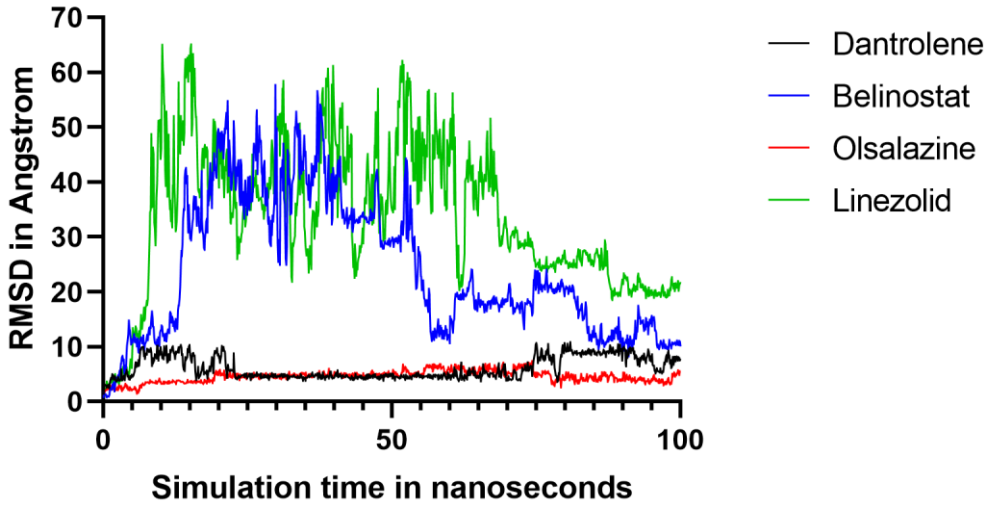

Figure 4: Ligand movement RMSD as a function of molecular dynamics (MD) simulation interval.

Table 3: Summary of molecular dynamics simulation results for selected hits.

No.	Drug name	Average MM-PBSA binding energy (Kcal/ mol)	Ligand movement RMSD (Å)		
			Mean	Minimum	Maximum
1	Dantrolene	-47.67	6.12	1.27	10.83
2	Belinostat	-6.58	24.06	0.69	57.66
3	Olsalazine	-113.97	4.59	1.11	7.37
4	Linezolid	-1.84	33.55	0.86	65.04

MM-PBSA: Molecular Mechanics Poisson-Boltzmann Surface Area**; RMSD:** Root-Mean-Square Deviation**; Å;** Angstrom.

Conclusion:

In this in silico study, we have used docking technique to screen a library of FDA approved drugs against NS2B-NS3 protease crystal of YFV. Then, the top hits with least energy of binding and capacity of hydrogen bonding with essential residues for protease activity were then evaluated by molecular dynamics simulation for 100 nanoseconds. Based on simulation output, Olsalazine was able to maintain a close proximity to protease active site as compared to Dantrolene, Belinostat and Linezolid. Also, Olsalazine had the least average MM-PBSA binding energy in contrast to the other three drugs. As such, Olsalazine may have the best potential to bind to and interfere with YFV protease activity. However, these in silico findings must be evaluated both in vitro and in vivo for further validation.

References:

1. RDV K, E M-D, T K, K W, B T, S H, et al. Yellow Fever: Integrating Current Knowledge with Technological Innovations to Identify Strategies for Controlling a Re-Emerging Virus. Viruses. 2019;11(10). DOI: 10.3390/V11100960

2. Monath TP. Yellow fever and dengue—the interactions of virus, vector and host in the re-emergence of epidemic disease. Semin Virol. 1994;5(2):133–45. DOI: 10.1006/SMVY.1994.1014

3. P S, P B, J B, EA G, G M, T M, et al. ICTV Virus Taxonomy Profile: Flaviviridae. J Gen Virol. 2017;98(1):2–3. DOI: 10.1099/JGV.0.000672

4. TP M, PF V. Yellow fever. J Clin Virol. 2015;64:160–73. DOI: 10.1016/J.JCV.2014.08.030

5. Tuboi SH, Costa ZGA, da Costa Vasconcelos PF, Hatch D. Clinical and epidemiological characteristics of yellow fever in Brazil: analysis of reported cases 1998–2002. Trans R Soc Trop Med Hyg. 2007;101(2):169–75. DOI: 10.1016/J.TRSTMH.2006.04.001

6. JJ W, A R, BA P. Yellow Fever Virus: Diagnostics for a Persistent Arboviral Threat. J Clin Microbiol. 2018;56(10). DOI: 10.1128/JCM.00827-18

7. EB H. Is it time for a new yellow fever vaccine? Vaccine. 2010;28(51):8073–6. DOI: 10.1016/J.VACCINE.2010.10.015

8. MUG K, NR F, RC R, N G, B N, S S, et al. Spread of yellow fever virus outbreak in Angola and the Democratic Republic of the Congo 2015-16: a modelling study. Lancet Infect Dis. 2017;17(3):330–8. DOI: 10.1016/S1473-3099(16)30513-8

9. I D, A H, R A, L C, A C, CA D, et al. International risk of yellow fever spread from the ongoing outbreak in Brazil, December 2016 to May 2017. Euro Surveill. 2017;22(28). DOI: 10.2807/1560-7917.ES.2017.22.28.30572

10. Furuse Y. Analysis of research intensity on infectious disease by disease burden reveals which infectious diseases are neglected by researchers. Proc Natl Acad Sci. 2019;116(2):478–83. DOI: 10.1073/PNAS.1814484116

11. TP M. Treatment of yellow fever. Antiviral Res. 2008;78(1):116–24. DOI: 10.1016/J.ANTIVIRAL.2007.10.009

12. CS de F, LM H, CQ S, AC F, PA R, R D, et al. Yellow fever virus is susceptible to sofosbuvir both in vitro and in vivo. PLoS Negl Trop Dis. 2019;13(1). DOI: 10.1371/JOURNAL.PNTD.0007072

13. GD N, VO G, RS F, ND F, MC B, G O, et al. Structural characterization and polymorphism analysis of the NS2B-NS3 protease from the 2017 Brazilian circulating strain of Yellow Fever virus. Biochim Biophys acta Gen Subj. 2020;1864(4). DOI: 10.1016/J.BBAGEN.2020.129521

14. A S, R P. Molecular targets for flavivirus drug discovery. Antiviral Res. 2009;81(1):6–15. DOI: 10.1016/J.ANTIVIRAL.2008.08.004

15. AS de G, R SF, AC CA, R VB, NC de MRM, RV CG, et al. Structural and mechanistic insight from antiviral and antiparasitic enzyme drug targets for tropical infectious diseases. Curr Opin Struct Biol. 2019;59:65–72. DOI: 10.1016/J.SBI.2019.02.014

16. AS R, H A, MJ M, R C-A, V A, T D. Recent applications of deep learning and machine intelligence on in silico drug discovery: methods, tools and databases. Brief Bioinform. 2019;20(5):1878–912. DOI: 10.1093/BIB/BBY061

17. Odhar HA, Ahjel SW, Albeer AAMA, Hashim AF, Rayshan AM, Humadi SS. Molecular docking and dynamics simulation of FDA approved drugs with the main protease from 2019 novel coronavirus. Bioinformation. 2020;16(3):236–44. DOI: 10.6026/97320630016236

18. Odhar HA, Ahjel SW, Odhar ZA. Computational Screening of FDA Approved Drugs from ZINC Database for Potential Inhibitors of Zika Virus NS2B/NS3 Protease: A Molecular Docking and Dynamics Simulation Study. J Pharm Res Int. 2021;33(39B):308–19. DOI: 10.9734/JPRI/2021/V33I39B32208

19. ZINC. Accessed 1 Oct 2021. Available: https://zinc.docking.org/

20. Sterling T, Irwin JJ. ZINC 15 - Ligand Discovery for Everyone. J Chem Inf Model. 2015;55(11):2324–37. DOI: 10.1021/ACS.JCIM.5B00559

21. mcule. Accessed 1 Oct 2021. Available: https://mcule.com/

22. RCSB PDB - 6URV: Crystal structure of Yellow Fever Virus NS2B-NS3 protease domain. Accessed 1 Oct 2021. Available: https://www.rcsb.org/structure/6URV

23. Noske GD, Gawriljuk VO, Fernandes RS, Furtado ND, Bonaldo MC, Oliva G, et al. Structural characterization and polymorphism analysis of the NS2B-NS3 protease from the 2017 Brazilian circulating strain of Yellow Fever virus. Biochim Biophys Acta - Gen Subj. 2020;1864(4). DOI: 10.1016/J.BBAGEN.2020.129521

24. Pettersen EF, Goddard TD, Huang CC, Couch GS, Greenblatt DM, Meng EC, et al. UCSF Chimera - A visualization system for exploratory research and analysis. J Comput Chem. 2004;25(13):1605–12. DOI: 10.1002/jcc.20084

25. Morris GM, Huey R, Lindstrom W, Sanner MF, Belew RK, Goodsell DS, et al. AutoDock4 and AutoDockTools4: Automated docking with selective receptor flexibility. J Comput Chem. 2009;30(16):2785–91. DOI: 10.1002/jcc.21256

26. Trott O, Olson AJ. AutoDock Vina: Improving the speed and accuracy of docking with a new scoring function, efficient optimization, and multithreading. J Comput Chem. 2009;31(2):NA-NA. DOI: 10.1002/jcc.21334

27. Drug, OTCs & Herbals | Medscape Reference. Accessed 1 Oct 2021. Available: https://reference.medscape.com/drugs

28. Laskowski RA, Swindells MB. LigPlot+: Multiple ligand-protein interaction diagrams for drug discovery. J Chem Inf Model. 2011;51(10):2778–86. DOI: 10.1021/ci200227u

29. Krieger E, Vriend G. YASARA View - molecular graphics for all devices - from smartphones to workstations. Bioinformatics. 2014;30(20):2981–2. DOI: 10.1093/bioinformatics/btu426

30. Krieger E, Dunbrack RL, Hooft RWW, Krieger B. Assignment of protonation states in proteins and ligands: Combining pK a prediction with hydrogen bonding network optimization. Methods Mol Biol. 2012;819:405–21. DOI: 10.1007/978-1-61779-465-0_25

31. Jakalian A, Jack DB, Bayly CI. Fast, efficient generation of high-quality atomic charges. AM1-BCC model: II. Parameterization and validation. J Comput Chem. 2002;23(16):1623–41. DOI: 10.1002/jcc.10128

32. Maier JA, Martinez C, Kasavajhala K, Wickstrom L, Hauser KE, Simmerling C. ff14SB: Improving the Accuracy of Protein Side Chain and Backbone Parameters from ff99SB. J Chem Theory Comput. 2015;11(8):3696–713. DOI: 10.1021/acs.jctc.5b00255

33. Wang J, Wolf RM, Caldwell JW, Kollman PA, Case DA. Development and testing of a general Amber force field. J Comput Chem. 2004;25(9):1157–74. DOI: 10.1002/jcc.20035

34. Hornak V, Abel R, Okur A, Strockbine B, Roitberg A, Simmerling C. Comparison of multiple amber force fields and development of improved protein backbone

parameters. Proteins Struct Funct Genet. 2006;65(3):712–25. DOI: 10.1002/prot.21123

35. Essmann U, Perera L, Berkowitz ML, Darden T, Lee H, Pedersen LG. A smooth particle mesh Ewald method. J Chem Phys. 1995;103(19):8577–93. DOI: 10.1063/1.470117

36. Krieger E, Vriend G. New ways to boost molecular dynamics simulations. J Comput Chem. 2015;36(13):996–1007. DOI: 10.1002/jcc.23899

37. JM S, RH H, JA M. Revisiting free energy calculations: a theoretical connection to MM/PBSA and direct calculation of the association free energy. Biophys J. 2004;86(1 Pt 1):67–74. DOI: 10.1016/S0006-3495(04)74084-9

38. C W, Y L, Y Y, P Z, W Z, Y W, et al. Analysis of therapeutic targets for SARS-CoV-2 and discovery of potential drugs by computational methods. Acta Pharm Sin B. 2020;10(5):766–88. DOI: 10.1016/J.APSB.2020.02.008

39. B J, S L, G L, H W. Could dantrolene be explored as a repurposed drug to treat COVID-19 patients by restoring intracellular calcium homeostasis? Eur Rev Med Pharmacol Sci. 2020;24(19):10228–38. DOI: 10.26355/EURREV_202010_23247

40. Elzupir AO. Inhibition of SARS-CoV-2 main protease 3CLpro by means of α-ketoamide and pyridone-containing pharmaceuticals using in silico molecular docking. J Mol Struct. 2020;1222:128878. DOI: 10.1016/J.MOLSTRUC.2020.128878

41. Loschwitz J, Jäckering A, Keutmann M, Olagunju M, Eberle RJ, Coronado MA, et al. Novel inhibitors of the main protease enzyme of SARS-CoV-2 identified via molecular dynamics simulation-guided in vitro assay. Bioorg Chem. 2021;111:104862. DOI: 10.1016/J.BIOORG.2021.104862

42. Amin SA, Ghosh K, Singh S, Qureshi IA, Jha T, Gayen S. Exploring naphthyl derivatives as SARS-CoV papain-like protease (PLpro) inhibitors and its implications in COVID-19 drug discovery. Mol Divers. 2021;1:1. DOI: 10.1007/S11030-021-10198-3

43. Tian D, Liu Y, Liang C, Xin L, Xie X, Zhang D, et al. An update review of emerging small-molecule therapeutic options for COVID-19. Biomed Pharmacother. 2021;137:111313. DOI: 10.1016/J.BIOPHA.2021.111313